


 Cite this: *Nanoscale*, 2020, **12**, 14472



Received 26th April 2020.

Accepted 22nd June 2020

DOI: 10.1039/d0nr03266b

rsc.li/nanoscale

Sandwiched graphene/hBN/graphene photonic crystal fibers with high electro-optical modulation depth and speed†

 Xu Cheng,^{‡a,b} Xu Zhou,^{‡a} Langyi Tao,^{‡a} Wentao Yu,^{‡a} Can Liu,^a Yi Cheng,^{c,d} Chaojie Ma,^a Nianze Shang,^a Jin Xie,^a Kaihui Liu ^{*a,e} and Zhongfan Liu ^{*c,d}

Graphene-photonic crystal fibers (PCFs) are obtained by integrating the broadband optical response and electro-optic tunability of graphene with the high-quality waveguide capacity and easy-integrability of the PCF, and this has been proven to be an important step towards multimaterial multifunctional fiber and all-fiber integrated circuits. However, the reported electro-optic modulator based on directly-grown graphene-PCF suffers from very low response speed (below 100 Hz) due to the slow response of ionic liquid. Here, we propose new functional PCFs with a sandwiched graphene/hBN/graphene (Gr/hBN/Gr) film attached to the hole walls of the fibers, and theoretically demonstrate that the in-line modulator based on it can achieve simultaneous single-mode transmission ranging from 1260 nm to 1700 nm (covering all optical communication bands), significant modulation depth (e.g. ~ 42 dB mm⁻¹ at 1550 nm) and high modulation speed (up to ~ 0.1 GHz). Furthermore, various device functions can be designed by changing the structure of the fiber, including the length, the hole diameter and the layer numbers of graphene and hBN films. This proposed approach directs a viable path to obtain high-performance all-fiber devices based on hybrid two-dimensional material optical fibers.

Photonic crystal fibers (PCFs), as a typical optical fiber with high-quality waveguide capacity and easy-integrability, have

established an excellent platform of photon manipulation for optical communication technology, and opened a window for exploring new functional fibers and fiber devices.^{1–8} In particular, they have been extensively studied to exploit diverse structures which possesses variable properties, such as endless single mode ability, high energy transmission, high nonlinear optical effect, *etc.* Since 2004, graphene has gained plenty of attention due to its potential applications in photonics and optoelectronics because of its many extremely fascinating properties, typically, including the markedly tunable electro-optical response that originates from its linear dispersion relationship and massless Dirac fermions.^{9–17} Naturally, the integration of graphene with optical fibers has great potential to both amplify advantages and unveil some new functions and devices, such as all-fiber electro-optical modulators, broadband polarizers, fiber sensors, ultrafast fiber lasers, *etc.*^{18–20} Among these, graphene-fiber electro-optical modulators based on the easily tunable electro-optical effect of graphene has received much attention. And many efforts have been devoted to achieve high performance, including coating graphene flakes on the side surface of polished or tapered optical fiber or filling them into the hollow fibers.^{21–24} But these architectures can break the transmission mode or original structures of the fibers, and still stay at the sample level, which results in fabrication difficulty and high production cost.

In a recent work,²⁵ a new kind of graphene optical fiber has been reported, which avoided these problems effectively, where graphene films are attached to the hole surface inside the PCF by the chemical vapor deposition growth method. Furthermore, by using the ionic liquid gating effect, the exploited electro-optical modulator based on graphene-PCF shows great performance with high modulation depth, broad wavelength range and low drive voltage. However, it still lacked high modulation speed due to the slow response speed (or the large time constant) of ionic liquid, although graphene has a potential ultrahigh response speed of ~ 500 GHz because of

^aState Key Laboratory for Mesoscopic Physics, School of Physics, Academy for Advanced Interdisciplinary Studies, Peking University, Beijing 100871, China. E-mail: khliu@pku.edu.cn

^bPhysical Science Laboratory, Huairou National Comprehensive Science Center, Beijing 101400, China

^cBeijing Graphene Institute (BGI), Beijing 100095, China. E-mail: zfliu@pku.edu.cn

^dCenter for Nanochemistry, College of Chemistry and Molecular Engineering, Peking University, Beijing 100871, China

^eFrontiers Science Center for Nano-optoelectronics, Collaborative Innovation Center of Quantum Matter, Beijing 100871, China

†Electronic supplementary information (ESI) available. See DOI: 10.1039/d0nr03266b

‡These authors contributed equally to this work.

the fast relaxation time of excited electrons.¹² This low modulation speed limits its real applications in all-fiber communication systems.

Here, we provide a feasible graphene-PCF modulator with high performance where graphene/hexagonal boron nitride/graphene (Gr/hBN/Gr) films are attached directly to the hole surface of PCF. By applying a relatively low external square-wave drive voltage on this capacitor-like Gr/hBN/Gr structure, the intensity of guided light can be rapidly modulated. Combined with the specially designed structure, this Gr/hBN/Gr PCF modulator can simultaneously achieve single mode transmission, broad optical communication wavelength (from O-band to U-band), significant modulation depth (e.g. ~ 42 dB mm^{-1} at 1550 nm), high modulation speed (up to ~ 0.1 GHz) and relatively low drive voltage (below 30 volts). The proposed

approach provides a promising new kind of graphene-integrated fiber device with high performance in all-fiber systems.

In this proposed hybrid PCF, four circles of air holes with equal diameter Φ and hole pitch Λ periodically surround the solid fiber core along the length direction and the Gr/hBN/Gr films are attached in an orderly manner to the hole surface (Fig. 1a). The Gr/hBN/Gr sandwiched structure along this hybrid PCF acts as an equivalent parallel-plate capacitor where two graphene films come in contact with two electrodes connected to a voltage source respectively, and the intensity of core-guided light is modulated by applying a small external square-wave drive voltage because of the electro-optical effect of graphene (Fig. 1a, right panel). The hBN film with a large bandgap (~ 6 eV) acts as an excellent electrical insulating and optical transparent material in this fiber modulator.

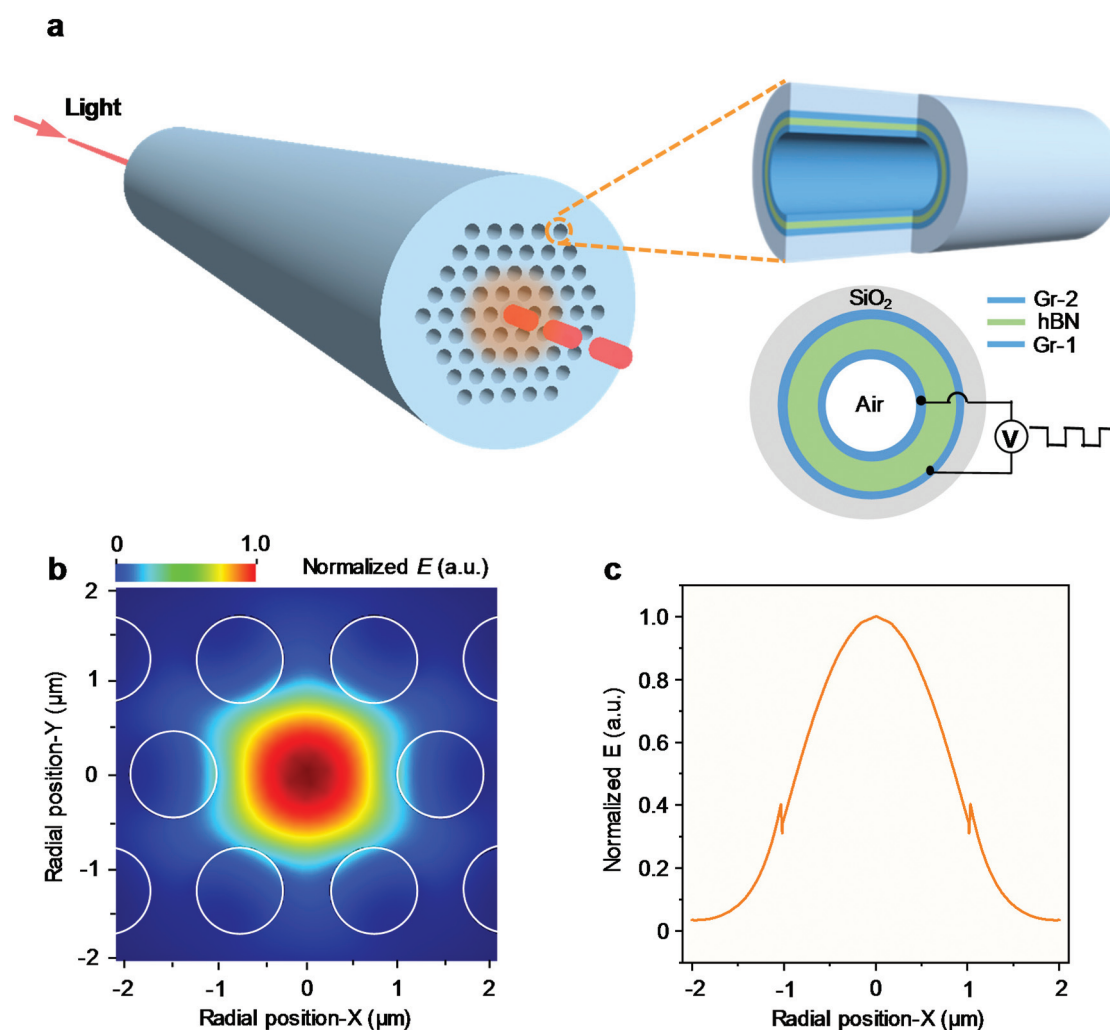


Fig. 1 Schematic illustration of a sandwiched Gr/hBN/Gr PCF modulator. (a) The surface of air holes of PCF (hole diameter and pitch are both on the micron scale) is fully covered with Gr/hBN/Gr films (details in the top right panel). The intensity of core-guided light in the PCF modulator can be modulated by applying a small external square-wave drive voltage to this capacitor-like Gr/hBN/Gr structure (bottom right panel). The two graphene films are marked as Gr-1 and Gr-2, respectively. (b) The electric field distribution in the fundamental guided mode in Gr/hBN/Gr PCF calculated by the finite element method. White circles highlight the air holes edge (hole diameter and pitch are $1 \mu\text{m}$ and $1.516 \mu\text{m}$, respectively) and monolayer hBN and two monolayer graphene films are attached to the hole surfaces in the PCF. (c) The normalized electric field intensity (E) of light in the Gr/hBN/Gr PCF along the radial position-X at the radial position-Y is equal to zero.

Considering the slight increase of the effective refractive index of cladding caused by the addition of Gr/hBN/Gr films with nanometer thickness, we elaborately design the dimensions of the hole diameter and hole pitch to guarantee single mode transmission to cover all optical communication bands based on the total internal reflection theory.²⁶ The large wavelength range of single mode transmission of the PCF combines faultlessly with the electrically tunable broadband optical response of graphene, which couldn't be better exploited as a broadband fiber modulator.

In Gr/hBN/Gr PCF, the transmitted light is confined in the solid fiber core in the form of fundamental guiding mode, just like the bare PCF (Fig. S1a†), and the electric field distribution of this mode is simulated by the finite element method based on full-vector Maxwell's equations (Fig. 1b). This method has higher accuracy in photonics modelling and is one of the most common method for simulating graphene-integrated waveguide devices.^{12,18,19} The mode field area spreading to the region of holes gives the obvious evidence that core-guided light interacts with graphene films by an evanescent wave at the interface between silica and Gr/hBN/Gr films, where the electric field relative intensity (ratio of light intensity at the innermost graphene position to that at the core center) becomes ~34.12% from ~34.06% of the bare PCF (Fig. S1b†). A distinct saltation of electric field intensity occurs at the interfaces between silica (or air) and Gr/hBN/Gr due to the sudden change in the refractive indices (real part of complex refractive indices of silicon, graphene,²⁷ hBN²⁸ and air are 1.444, 2.934, 1.8 and 1.0, respectively), indicating the direct strong light-graphene interaction (Fig. 1c). Here the refractive index for few-layer graphene remains constant with different layer numbers^{18,29} and we use a constant infrared refractive index for both hBN film and bulk.²⁸ Considering the weak van der Waals interaction at the graphene-hBN interface, we treat them as two separated materials in the simulation.³⁰ Material parameters including the refractive index in our article are listed in ESI Table.†

The strong light-graphene interaction can be further demonstrated by the large transmission attenuation coefficient (A_t) of up to 42.4 dB mm⁻¹ in the Gr/hBN/Gr PCF ($\Phi = 1 \mu\text{m}$ and $\Lambda = 1.516 \mu\text{m}$, single layer graphene and hBN film), as the fitted slope of length dependent light transmission attenuation shown in Fig. 2a. In contrast to the ignorable attenuation of bare PCF, this transmission attenuation is totally caused by graphene absorption, which can be exactly tuned from the absorbing state to an entirely transparent state and further utilized as a modulator of the electro-optical effect of graphene. In this case, the attenuation of Gr/hBN/Gr PCF is in theory the numeric equivalent of the largest modulation depth of the fiber modulator. The strong attenuation obviously depends on the thickness of graphene as well as the fiber length. As shown in Fig. 2b, the light transmission attenuation coefficient of the Gr/hBN/Gr PCF is linearly dependent on the layer number of the bottom and top graphene films N_{Gr} (the layer number of two graphene films are always set to be the same artificially) because of the weak van der Waals interaction between the graphene layers.²⁹ From the fitting straight line, the attenuation

coefficient can be expressed as $A_t(N_{\text{Gr}}) = 42.1 \times N_{\text{Gr}} \text{ dB mm}^{-1}$ where the slope reveals the uniform electric field in graphene layers under its thin thickness (less than 10 layers, Fig. S2a†).

On the other hand, the layer number of hBN films (N_{hBN}) naturally changes the light intensity distribution (Fig. S2b†), which results in a slow nonlinear increase of the attenuation coefficient with N_{hBN} (Fig. 2c), that is, $A_t(N_{\text{hBN}}) = 2.4 \times (1 + N_{\text{hBN}}/100)^2 + 40 \text{ dB mm}^{-1}$. Besides, reducing the air hole diameter Φ is also an efficient way to enhance the light-graphene interaction or transmission attenuation coefficient ($A_t(\Phi) = 42.4 \times \Phi^{-4.1} \text{ dB mm}^{-1}$) under the condition of the invariable single mode transmission range (wavelength >1260 nm) (Fig. 2d). The reason is that the diminution of air hole can enhance the relative intensity of the Gr/hBN/Gr PCF structure (Fig. S2c†). Considering all of these factors together, the total light transmission attenuation coefficient, *i.e.* the maximum modulation depth of this fiber modulator, can be quantitatively defined as:

$$A_t(N_{\text{Gr}}, N_{\text{hBN}}, \Phi) = N_{\text{Gr}} \Phi^{-4.1} [2.4 \times (1 + N_{\text{hBN}}/100)^2 + 40] \text{ dB mm}^{-1}.$$

Based on the clear relationship between strong light-graphene interaction and structure, we can naturally make the Gr/hBN/Gr PCF with such strong and tunable light-matter interaction an in-line electro-optical modulator in all-fiber communication networks. In the modulator as illustrated in Fig. 1a, two leads from a voltage source connect the two graphene films in the sandwiched Gr/hBN/Gr structure respectively, where the light intensity is modulated by applying a small external square-wave drive voltage. The external drive voltage V_{dr} shifts the graphene Fermi level (E_{F}) up or down from the neutral point, according to the electro-optical effect of graphene. When the Fermi level shift is smaller (larger) than half of the incident photon energy ($\hbar\omega/2$), graphene can (cannot) absorb the photon because of the occupied conduction band (Pauli exclusion principle) or unavailable valence band (Fig. 3a). As an example (Fig. 3b-d), the fiber modulator ($\Phi = 1 \mu\text{m}$, $\Lambda = 1.516 \mu\text{m}$ and $1N_{\text{Gr}} = N_{\text{hBN}} = 1$) can work with single mode transmission from 1260 to 1700 nm and high modulation depth from 35 to 50 dB mm⁻¹ by shifting the E_{F} (corresponding to theoretical drive voltage from 28.3 to 15.6 V, ESI Note S1†). At the typical communication wavelength of 1550 nm, the modulator works from the off state (absorption) to the on state (transparency) with modulation depth from 0 to ~42 dB mm⁻¹ when the E_{F} shifts from the neutral point (Fig. 3c). Furthermore, such a fiber modulator can work at a broad wavelength range of 1260–1700 nm with single mode transmission, where the modulation depth increases markedly with wavelength for the increase of the real and imaginary part of graphene refractive index and consequently enhanced light-graphene interaction (Fig. 3d).

Except the modulation depth, wavelength range and drive voltage, the operating bandwidth is another important performance parameter. Just like other electro-optical modulators, the bandwidth of the Gr/hBN/Gr PCF modulator $f = 1/(2\pi RC)$ is also mainly limited by the response time constant of the equivalent circuit (Fig. 4a). The effective total resistance R and capaci-

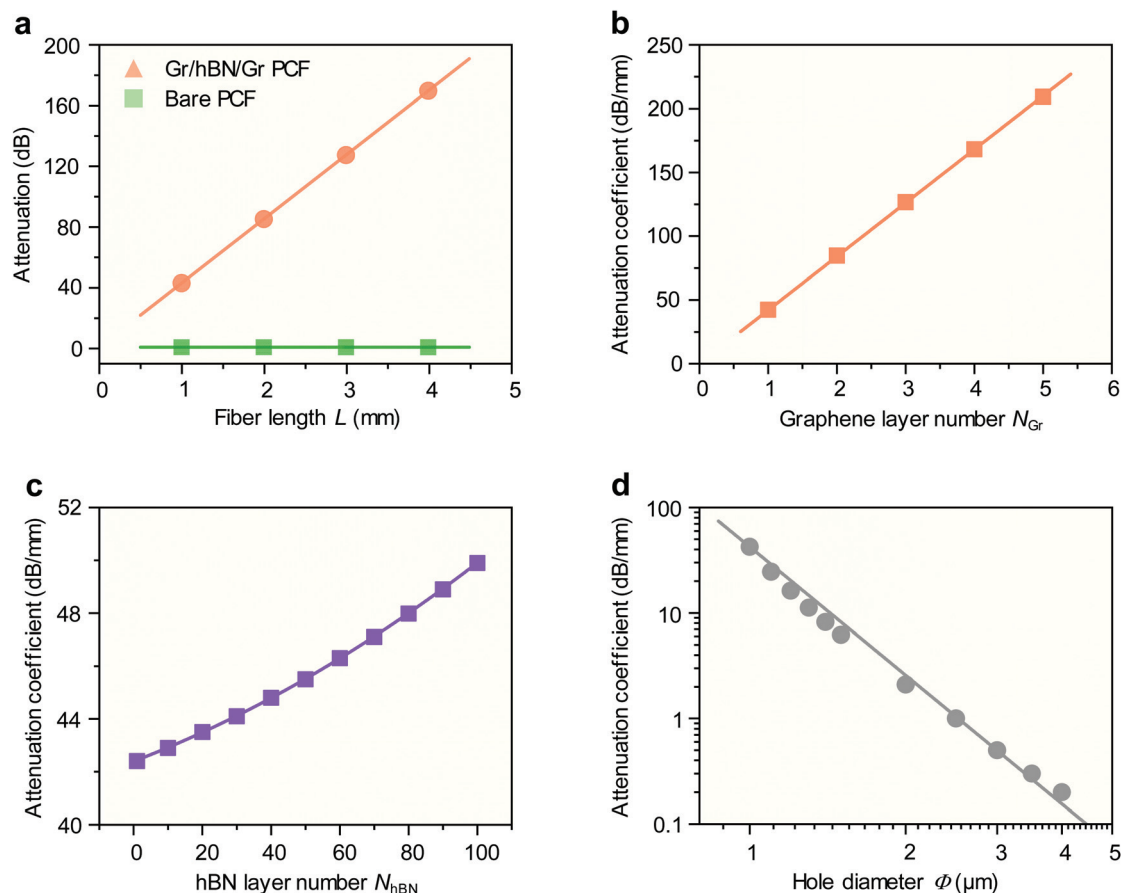


Fig. 2 Light–graphene interaction of the Gr/hBN/Gr PCF. (a) The dependence of propagation attenuation of incident light on the length of bare PCF (green) and Gr/hBN/Gr PCF (orange, monolayer hBN and two monolayer graphene, hole diameter of 1 μm and hole pitch of 1.516 μm). The linear fitting curve with an $\sim 42 \text{ dB mm}^{-1}$ slope indicates a strong light–matter interaction. The nearly invariable attenuation data of the bare PCF shows a negligible light intensity attenuation and stable low insertion loss as well. (b–d) Based on the data in (a), the light attenuation coefficient with single mode transmission upon changing only the graphene layer number N_{Gr} (b), hBN layer number N_{hBN} (c) and air hole diameter ϕ (d), respectively. Single mode transmission is guaranteed with different ϕ and hole pitch λ in (d). All the dots and lines correspond to the simulated data and fitting curves, respectively.

tance C show close relationship with the fiber length L , thickness of hBN films d , carrier concentration n in graphene films, *etc.* Here, the operating bandwidth can be simplified as below (ESI Note S2†), including the quantum capacitance and the resistance variable of graphene with the carrier concentration n :

$$f = \frac{d + \frac{\epsilon \hbar v_F \sqrt{\pi}}{e^2} \times \frac{1}{\sqrt{n}}}{4\pi\epsilon L^2 \left(R_{s\infty} + \frac{1}{ne\mu_C + 1/R_{s0}} \right)}$$

$$\approx \frac{d + 0.23 \times \frac{1}{\sqrt{n}}}{L^2 \left(4.4 + \frac{1.4 \times 10^{17}}{n + 3.3 \times 10^{15}} \right)} \times 10^8 \text{ Hz},$$

where ϵ , e , π , \hbar , v_F and μ_C are respectively the permittivity constant of hBN, electron charge, circular constant, reduced Planck constant, Fermi velocity and the carrier concentration-independent carrier mobility corresponding to the long-range scattering, and $R_{s\infty}$ and R_{s0} are respectively the resistance $n \rightarrow \infty$ induced by the

short-range scattering and the residual resistance at the Dirac point of the graphene film. The influence of the hBN substrate on graphene plates is reflected on the sheet resistance of graphene.³⁰ Obviously, this indicates that broader bandwidth has close relationship with shorter fiber length L and larger thickness of hBN ($d = 0.34 \times N_{hBN} \text{ nm}$).

At the same time, the drive voltage is also mainly limited by the thickness of the hBN film where the Gr/hBN/Gr films acts as a capacitor (Fig. 4a and ESI Note S1†). Furthermore, lower voltage is always preferable for low-energy integration in practical application. Therefore, combining the previous analysis, the hBN thickness d is incompatible for achieving the low voltage, high modulation depth and large bandwidth. Taking all these factors into consideration, we take an example of a PCF modulator with 100-layer hBN ($\sim 34 \text{ nm}$ thickness) and two monolayer graphene films. In this situation, the modulator can work with drive voltages below 30 volts, modulation depth of $\sim 42 \text{ dB mm}^{-1}$ at 1550 nm and single mode transmission covering all optical communication bands from 1260 to 1700 nm. The dependence of the modulator on the band-

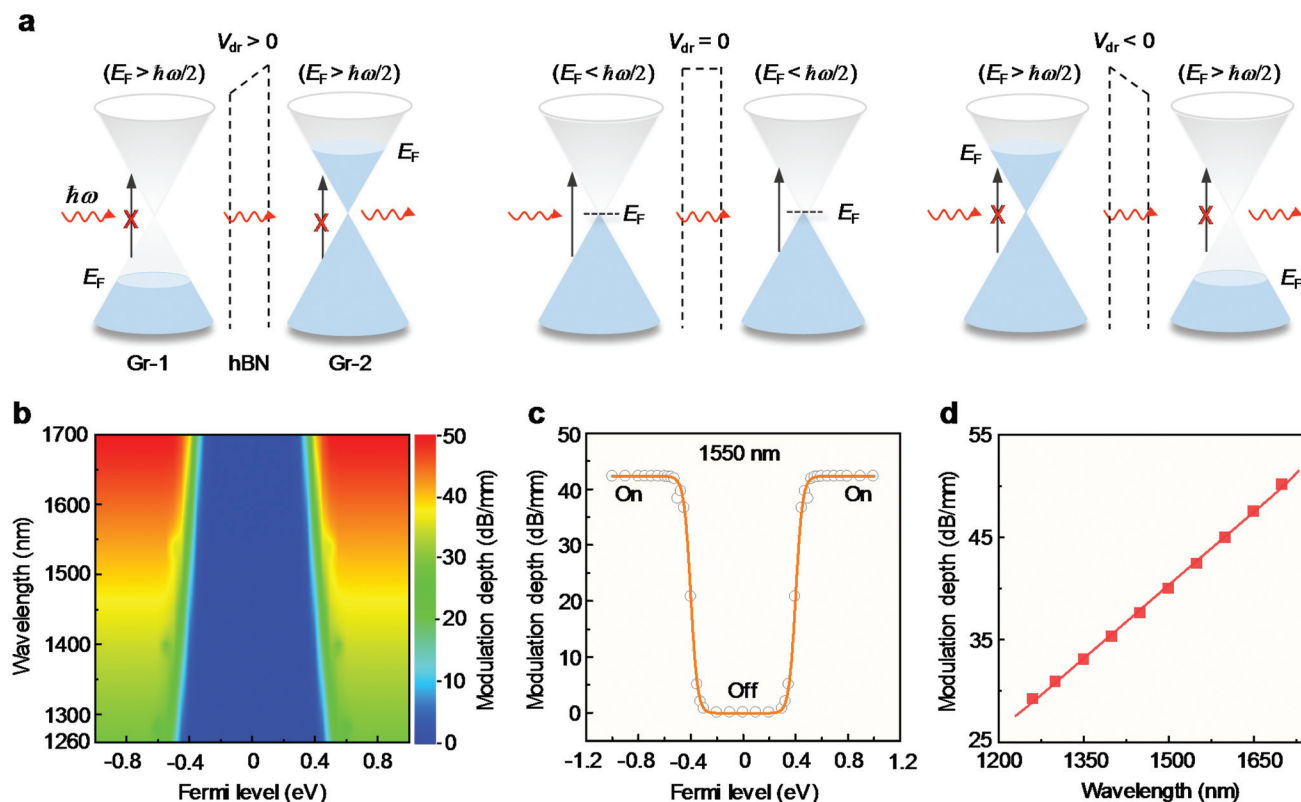


Fig. 3 Electro-optic modulation of the Gr/hBN/Gr PCF modulator. (a) The simplified electrical band structures and the electrically-tuned E_F of graphene (dashed lines show the voltage drop caused by the external drive voltage V_{dr}). The incident photons (red) can (or can't) be absorbed by the Gr/hBN/Gr PCF if the $E_F < \hbar\omega/2$ (or $E_F > \hbar\omega/2$), because of the Pauli exclusion principle. (b) The modulation depth varies at different Fermi levels and working wavelengths (1260–1700 nm). (c) The modulation curve of the modulator at 1550 nm (extracted from (b)) shows an unambiguous transition between the on and off state. (d) Modulation depth at different working wavelength ranges (extracted from (b)). In this modulator, monolayer hBN and two monolayer graphene films are attached to the holes surface where the hole diameter and pitch are 1 μm and 1.516 μm , respectively.

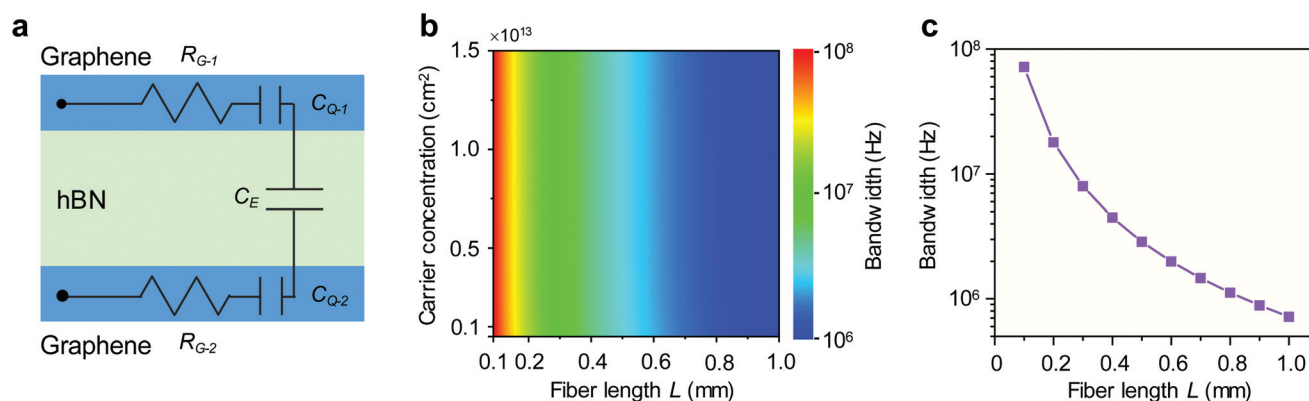


Fig. 4 Modulation bandwidth of the Gr/hBN/Gr PCF modulator. (a) Schematic of the equivalent circuit of the Gr/hBN/Gr capacitor consisting of the graphene resistances (R_{G-1} and R_{G-2}) and quantum capacitances (C_{Q-1} and C_{Q-2}) of two graphene films (blue) and the capacitance (C_E) of the hBN film (green). (b) The bandwidth of this modulator as a function of carrier concentration of graphene and fiber length at a working wavelength of 1550 nm. (c) The bandwidth of the Gr/hBN/Gr PCF modulator shows an inverse relationship with the fiber length when the graphene carrier concentration is $\sim 9.7 \times 10^{12} \text{ cm}^{-2}$ (extracted from (b)). In this modulator, 100-layer hBN and two monolayer graphene films are attached to the holes surface where the hole diameter and pitch are 1 μm and 1.516 μm , respectively.

width, wavelength and fiber length is mapped, as shown in Fig. 4b and c, which directly indicates that the modulator with the fiber length ranging from 1 to 0.1 mm can achieve 1 MHz–

0.1 GHz bandwidth regardless of the graphene carrier concentration varying from 1.5×10^{13} to $8.1 \times 10^{11} \text{ cm}^{-2}$. Although the graphene carrier concentration is directly tuned by the E_F and

indirectly changed by the drive voltage,³¹ the operating bandwidth is unaffected by the carrier concentration or drive voltage. Moreover, the operating bandwidth shows little variation in the broad wavelength range (Fig. S3a†), but is greatly affected by the fiber length (Fig. 4c) resulting from the significant dependence of the resistance and capacitance of the Gr/hBN/Gr structure on the fiber length and slight changes in these with the carrier concentration. And it grows nearly linearly with hBN thickness due to a linear change in the structure capacitance which dominates the capacitance C (Fig. S3b†). The fiber length and hBN thickness, in a word, are both directly related with the effective total resistance R and capacitance C (*i.e.* the response time), and subsequently influence the operating bandwidth.

In theoretical analysis, we consider an ideal single crystal graphene/hBN/graphene structure. But in actual situation, defects or impurities and problems attached to them such as change in the electronic structure are inevitable and it would certainly decrease the device performance. With the development of low-dimensional material manufacture technology, it is worth looking forward to that the impact of these problems will definitely get better. For example, the efforts made toward ultraclean graphene synthesis with less defects, high mobility and low resistance is one of the effective way to overcome this problem.^{32,33}

In summary, we theoretically provided a technically achievable all-fiber electro-optical modulator based on sandwiched Gr/hBN/Gr PCFs. Our hybrid fiber modulator exhibits single-mode transmission ranging from 1260 nm to 1700 nm, significant modulation depth (*e.g.* ~ 42 dB mm^{-1} at 1550 nm) and high modulation speed (up to ~ 0.1 GHz), simultaneously. In addition, various required performance indicators can be achieved by changing the structure, including the fiber length, the fiber hole diameter and the layer numbers of the graphene and hexagonal boron nitride films. We anticipate that such specially designed Gr/hBN/Gr PCF architectures can be operational and realized by the chemical vapor deposition method based on reported technologies where the graphene/hBN heterojunction³⁴ and graphene-PCF²⁵ both have been successfully achieved. Our strategy provides a straightforward design for a new kind of all-fiber electro-optical modulator with high performance that is likely to find its applications in future all-fiber system.

Author contributions

X.C., X.Z., L.T. and W.Y. contributed equally to this work. Z.L. and K.L. supervised the project. K.L. and X.Z. conceived the project. X.C. performed theoretical modelling. L.T. calculated the electric properties. X.Z., W.Y., C.L., C.M., N.S. and J.X. investigated the optical modulator. Y.C. suggested the material growth theory. X.Z., X.C. and L.T. wrote the manuscript. All authors contributed to the scientific discussion on the manuscript.

Conflicts of interest

There are no conflicts to declare.

Acknowledgements

This work was supported by the Beijing Natural Science Foundation (JQ19004), the Beijing Graphene Innovation Program (Z181100004818003), the National Natural Science Foundation of China (51991340, 51991342, 51522201 and 51520105003), the National Key R&D Program of China (2016YFA0300903, 2016YFA0200103 and 2016YFA0300804), the Beijing Excellent Talents Training Support (2017000026833ZK11), the Beijing Municipal Science & Technology Commission (Z191100007219005), the Key R&D Program of Guangdong Province (2020B010189001, 2019B010931001, and 2018B030327001), the Bureau of Industry and Information Technology of Shenzhen (201901161512), the National Postdoctoral Program for Innovative Talents (BX20180013 and BX20190016), and the China Postdoctoral Science Foundation (2019M660001 and 2019M660280).

References

- 1 P. Russell, Photonic crystal fibers, *Science*, 2003, **299**, 358–362.
- 2 J. C. Knight, Photonic crystal fibres, *Nature*, 2003, **424**, 847–851.
- 3 D. G. Ouzounov, F. R. Ahmad, D. Muller, *et al.*, Generation of megawatt optical solitons in hollow-core photonic band-gap fibers, *Science*, 2003, **301**, 1702–1704.
- 4 J. M. Dudley and J. R. Taylor, Ten years of nonlinear optics in photonic crystal fibre, *Nat. Photonics*, 2009, **3**, 85–90.
- 5 C. Markos, J. C. Travers, A. Abdolvand, *et al.*, Hybrid photonic-crystal fiber, *Rev. Mod. Phys.*, 2017, **89**, 045003.
- 6 A. F. Abouraddy, M. Bayindir, G. Benoit, *et al.*, Towards multimaterial multifunctional fibres that see, hear, sense and communicate, *Nat. Mater.*, 2007, **6**, 336–347.
- 7 R. He, P. J. A. Sazio, A. C. Peacock, *et al.*, Integration of gigahertz-bandwidth semiconductor devices inside microstructured optical fibres, *Nat. Photonics*, 2012, **6**, 174–179.
- 8 F. Köttig, D. Novoa, F. Tani, *et al.*, Mid-infrared dispersive wave generation in gas-filled photonic crystal fibre by transient ionization-driven changes in dispersion, *Nat. Commun.*, 2017, **8**, 813.
- 9 F. Bonaccorso, Z. Sun, T. Hasan, *et al.*, Graphene photonics and optoelectronics, *Nat. Photonics*, 2010, **4**, 611–622.
- 10 Q. Bao and K. P. Loh, Graphene photonics, plasmonics, and broadband optoelectronic devices, *ACS Nano*, 2012, **6**, 3677–3694.
- 11 F. Xia, H. Wang, D. Xiao, *et al.*, Two-dimensional material nanophotonics, *Nat. Photonics*, 2014, **8**, 899–907.
- 12 M. Liu, X. Yin, E. Ulin-Avila, *et al.*, A graphene-based broadband optical modulator, *Nature*, 2011, **474**, 64–67.

- 13 C. T. Phare, Y.-H. D. Lee, J. Cardenas, *et al.*, Graphene electro-optic modulator with 30 GHz bandwidth, *Nat. Photonics*, 2015, **9**, 511–514.
- 14 E. O. Polat and C. Kocabas, Broadband optical modulators based on graphene supercapacitors, *Nano Lett.*, 2013, **13**, 5851–5857.
- 15 M. Ono, M. Hata, M. Tsunekawa, *et al.*, Ultrafast and energy-efficient all-optical switching with graphene-loaded deep-subwavelength plasmonic waveguides, *Nat. Photonics*, 2020, **14**, 37–43.
- 16 T. Jiang, D. Huang, J. Cheng, *et al.*, Gate-tunable third-order nonlinear optical response of massless Dirac fermions in graphene, *Nat. Photonics*, 2018, **12**, 430–436.
- 17 H. Lin, Y. Song, Y. Huang, *et al.*, Chalcogenide glass-on-graphene photonics, *Nat. Photonics*, 2017, **11**, 798–805.
- 18 Q. Bao, H. Zhang, B. Wang, *et al.*, Broadband graphene polarizer, *Nat. Photonics*, 2011, **5**, 411–415.
- 19 E. J. Lee, S. Y. Choi, H. Jeong, *et al.*, Active control of all-fibre graphene devices with electrical gating, *Nat. Commun.*, 2015, **6**, 6851.
- 20 Y.-H. Lin, C.-Y. Yang, J.-H. Liou, *et al.*, Using graphene nano-particle embedded in photonic crystal fiber for evanescent wave mode-locking of fiber laser, *Opt. Express*, 2013, **21**, 16763–16776.
- 21 W. Li, B. Chen, C. Meng, *et al.*, Ultrafast all-optical graphene modulator, *Nano Lett.*, 2014, **14**, 955–959.
- 22 J. Chen, B. Zheng, G. Shao, *et al.* An all-optical modulator based on a stereo graphene-microfiber structure, *Light: Sci. Appl.*, 2015, **4**, e360.
- 23 H. Zhang, N. Healy, L. Shen, *et al.* Enhanced all-optical modulation in a graphene-coated fibre with low insertion loss, *Sci. Rep.*, 2016, **6**, 23512.
- 24 Y. Xiao, J. Zhang, J. Yu, *et al.*, Theoretical investigation of optical modulators based on graphene-coated side-polished fiber, *Opt. Express*, 2018, **26**, 13759–13772.
- 25 K. Chen, X. Zhou, X. Cheng, *et al.*, Graphene photonic crystal fibre with strong and tunable light-matter interaction, *Nat. Photonics*, 2019, **13**, 754–759.
- 26 M. D. Nielsen and N. A. Mortensen, Photonic crystal fiber design based on the V-parameter, *Opt. Express*, 2003, **11**, 2762–2768.
- 27 A. Vakil and N. Engheta, Transformation optics using graphene, *Science*, 2011, **332**, 1291.
- 28 S. Kim, J. Fröch, J. Christian, *et al.*, Photonic crystal cavities from hexagonal boron nitride, *Nat. Commun.*, 2018, **9**, 2623.
- 29 R. R. Nair, P. Blake, A. N. Grigorenko, *et al.*, Fine structure constant defines visual transparency of graphene, *Science*, 2009, **320**, 1308.
- 30 C. R. Dean, A. F. Young, I. Meric, *et al.*, Boron nitride substrates for high-quality graphene electronics, *Nat. Nanotechnol.*, 2010, **5**, 722–726.
- 31 A. Das, S. Pisana, B. Chakraborty, *et al.*, Monitoring dopants by Raman scattering in an electrochemically top-gated graphene transistor, *Nat. Nanotechnol.*, 2008, **3**, 210–215.
- 32 L. Zheng, Y. Chen, N. Li, *et al.*, Robust ultraclean atomically thin membranes for atomic-resolution electron microscopy, *Nat. Commun.*, 2020, **11**, 541.
- 33 L. Lin, J. Zhang, H. Su, *et al.*, Towards super-clean graphene, *Nat. Commun.*, 2019, **10**, 1912.
- 34 W. Yang, G. Chen, Z. Shi, *et al.*, Epitaxial growth of single-domain graphene on hexagonal boron nitride, *Nat. Mater.*, 2013, **12**, 792–797.